Efficient Computational Model of Phase Noise and its Applicability to Assess the Performance of Digital Modulation Techniques

Asmaa E. Farahat and Khlaid F. A. Hussein

Microwave Engineering Department
Electronics Research Institute, Cairo, 11843, Egypt
asmaa@eri.sci.eg, Khalid_elgabaly@yahoo.com

Abstract ─ Two methods are proposed to get a discrete-time model for a sinusoidal carrier signal affected by phase noise of a predetermined power spectral density (PSD). The proposed methods aim to calculate the instantaneous phase error at the discrete time samples. In the first method, uncorrelated uniformly distributed random numbers are generated at the discrete time samples and added to the angle of the carrier. These phase samples are, then, correlated along the time by enforcing the spectrum of the signal to take the magnitudes obtained from the predetermined PSD. In the second method, uniformly distributed random numbers are generated at the discrete frequencies which are uncorrelated along the frequency to represent the phase of the signal spectrum. In both methods, a subsequent application of the inverse Fourier transform results in the time domain waveform of the signal in which the time samples of the phase error appear as correlated random values. The instantaneous phase error is calculated for different ratios of the noise-to-carrier power. Experimental measurements of the PSD of the phase noise for some commercially available microwave generators are performed and the measurements are used to calculate the instantaneous phase error associating the output signal. In all the cases, the obtained phase noise model is used to study the effect of such a noise type on the performance of M-ary PSK communication systems where the dependence of the bit-error-rate on the noise-to-carrier power level is investigated.

Index Terms ─ M-ary PSK, phase error, phase noise.

I. INTRODUCTION

The growing capacity and quality demands in wireless communication systems imposed more stringent requirements on the accurate assessment and modeling of the phase noise of local oscillators. Even in the digital world, phase noise in the guise of jitter is important. Clock jitter directly affects timing margins and hence limits system performance. Phase noise causes spectral purity degradation which leads to channel interference in RF communication channels. In OFDM systems, Phase noise has two detrimental effects on the performance. It rotates all the subcarriers in the same OFDM symbol with a common phase, which is called common phase error (CPE). The more important is that it destroys the orthogonality of the subcarriers by spreading the power from one subcarrier to the adjacent subcarriers which is called inert-carrier interference [1]. In digital modulation techniques specially those employing phase to encode data as in PSK communication systems, it reduces the distance between the symbols leading to higher error rates. Phase noise in oscillators is one of the hardware impairments that is becoming a limiting factor in high data rate digital communication systems. It limits the performance of systems that employ dense constellations. Moreover, the level of phase noise at a given offset frequency increases with increasing the carrier frequency, which means that the phase noise problems may be worse in systems with high frequency carriers [1].

Phase noise is random phase fluctuations in a waveform. The fluctuations are visualized as sidebands in the signal power spectrum spreading out on either side of the signal. It reduces in level with increasing offset from the carrier frequency and is typically measured in dBc/Hz [1]. Phase noise is of particular importance as it reduces the quality of the signal and thus increases the rate of error in a communication link.

Phase noise is a phenomenon that essentially spreads out the power in a carrier. The carrier has no longer a discrete line power spectrum but a continuous PSD. The phase noise plot is a single side spectrum indicating the noise power density in one hertz bandwidth with regard to the carrier power. It can be modeled using power-law noise processes [2-4]. Phase noise typically rises much faster closer to the carrier and falls away as we get far from the carrier [5]. Power law noise processes are characterized by their functional dependence on Fourier frequencies. The spectral density plot of a typical oscillator's output is usually a combination of different power-law noise processes. It is very useful and meaningful to categorize the noise processes. The first job in evaluating a spectral density plot is to determine which type of noise exists for a particular

Submitted On: June 1, 2019
Accepted On: October 23, 2019

range of Fourier frequencies.

Several attempts to model phase noise have been reported in literature [6]-[12]. In [6], the oscillator phase noise is represented as integration of two functions representing flicker noise and white noise assuming independent noise sources. In [7], the phase noise is modeled as accumulated and synchronous random phase deviations with Gaussian distribution. It also relates the PSD of a noisy periodic signal analytically to its phase deviations which can be estimated from the jitter of the signal. In [8], flicker noise is estimated from white noise using the method of fractional order of integration. In [9], the phase noise is modeled as a random walk stochastic process added as random phase term to a sine wave and the decrease in sideband power is calculated when the oscillator signal is coherently mixed with a time delay replica of itself. In [10], a non-linear equation for the phase error is derived which is solved for the random phase perturbations. In [11] a power law model is used to model the phase noise with Gaussian stochastic process to represent the noise sources and a random variable representing the slope of each process. In [12] an analytic model for phase noise is derived to account for two sources of phase noise, thermo-mechanical and white noise.

In this work, the phase error range is estimated explicitly for phase noise characterized by its single side band PSD. A mathematical model for the phase noise is developed which enables the determination of the phase error span and instantaneous time samples. All the sources of phase noise can be accounted for in the proposed phase noise model accurately. Each of the previously mentioned methods has modeled certain types of phase noise sources but not all the sources that can be present in practical cases. Experimental measurements of the PSD of the phase noise for some commercially available microwave generators are performed and the instantaneous phase error associating the output signal is calculated. The effects of the phase noise on the performance of communication systems employing PSK modulation techniques are studied. The bit error rate (BER) and symbol rate (SER) can then be estimated for specific PSD of the phase noise.

II. MODELING THE PHASE NOISE

There are several types of phase noise, each characterized by the slope of the PSD curve. Phase noise across a range of frequencies will be dominated by a specific noise process [13]. In the present work it is considered that the oscillator may suffer from all or some of the following causes of phase noise, (i) *Random walk FM noise* $(1/f^4)$ found at lower offset frequencies, (ii) *flicker frequency noise* $(1/f^3)$, (iii) *white frequency noise* $(1/f^2)$ [14], (iv) *flicker PM noise* $(1/f)$[15], and (v) *white PM noise* $(1/f^0)$, which is mainly caused by thermal noise and shot noise [3]. It is possible to consider that all the five noise processes are generated from a single oscillator, but usually, only two or three noise processes are dominant. Figure 1 is a graph of single sideband PSD of a sinusoidal signal affected by phase noise on a log-log scale with all the five noise processes taken into consideration.

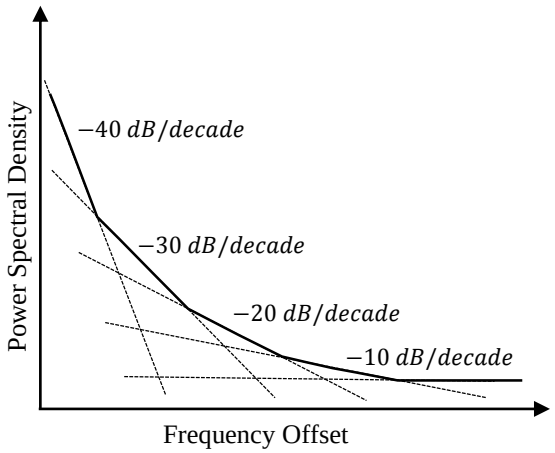

Fig. 1. Single side band PSD $L(f)$ describing phase noise characteristics.

The phase noise in the frequency domain is commonly characterized by the single side band PSD, $L(f)$, which is defined as the noise power in 1 Hz bandwidth at an offset frequency, f, from the carrier frequency relative to the carrier power [16, 17]:

$$L(f) = \frac{\text{Noise power in 1Hz bandwidth}}{P_c}, \qquad (1)$$

where P_c is the carrier power.

The magnitudes of the spectrum of a carrier signal affected by phase noise can be obtained as follows:

$$A(f) = \sqrt{P_c\, L(f)}. \qquad (2)$$

The spectrum of a pure sinusoidal signal is a Dirac delta function. The presence of phase noise will cause spectrum broadening as shown in Fig. 2. The noise-to-carrier power ratio (NCR) in a bandwidth Δf centered at the carrier frequency can be calculated as follows:

$$\text{NCR} = 2\int_0^{\Delta f/2} L(f)\, df. \qquad (3)$$

The PSD of the phase noise, $L(f)$ can be described by equation (1) according to the explained physical sources. This gives rise to the magnitude distribution $A(f)$ given by equation (2). However, the phase of the noisy signal, $\psi(f)$, and the instantaneous phase error in the time domain, $\varphi_e(t)$, are not known. The knowledge of the discrete-time phase errors, $\varphi_e(t_n)$, $n = 1,2,3,\cdots,N$, are

necessary whenever it is required to assess communication system performance measure such as the bit error rate (BER). The next section aims to evaluate the phase errors as functions of the frequency and time as well.

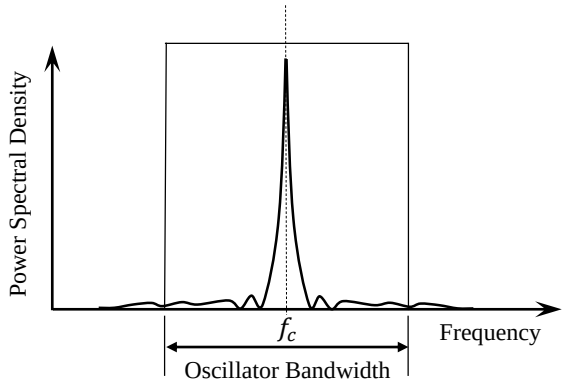

Fig. 2. Spectrum of a sinusoidal signal affected by phase noise.

For performance assessment in many applications including communication systems, it is necessary to determine the instantaneous phase error of a carrier signal subjected to phase noise. Modeling the phase noise means to get complete numerical information about a carrier signal affected by phase noise of a given PSD distribution. Complete information include the magnitude and phase distributions over the frequency for the carrier signal when affected by the phase noise, and also give the time samples of the signal from which the instantaneous phase error can be deduced.

In the first method, the phase noise is modeled through the following steps. First a random sequence of uniformly distributed random phase samples is generated and added to the angle of the carrier signal in time domain. The Fourier transformation is applied to the carrier signal where the magnitudes of the resulting signal spectrum are replaced by the magnitudes $A(f)$ which are obtained from $L(f)$ as given by (2). This process has the effect of correlating the random phase error samples along the time. The inverse Fourier transformation is, then, applied giving rise to the correlated time samples of the instantaneous phase error caused by the phase noise.

At high frequencies (in the gigahertz range) the above method may be impractical as it requires huge number of time and frequency samples to perform the Fourier transform which is memory and time consuming. An alternative procedure is proposed to construct the model of such a carrier signal with less computational complexity. This procedure starts with the construction of the magnitude and phase distribution in the frequency domain for the noisy carrier signal and then the inverse Fourier transform is applied to get the corresponding time samples. It should be noted that the magnitudes are obtained from the $L(f)$ as given by (2) whereas the phases (of the signal spectrum) are constructed as uniformly distributed random numbers in the range $[-\pi, \pi]$, which are not correlated along the frequency.

The following subsections provide descriptions for the two methods mentioned above to construct a model for the phase noise when affects a carrier signal.

A. Modeling phase noise as correlated time sequence of random phase errors

Let the carrier signal $\xi(t)$ without the phase noise be expressed as:

$$\xi(t) = A_c\, e^{j(2\pi f_c t + \Psi)}, \tag{4}$$

where A_c is the carrier amplitude, f_c is the carrier frequency, and Ψ is a constant phase. When such carrier signal is affected by phase noise, it can be expressed as:

$$s(t) = A_c \mathrm{e}^{j(2\pi f_c t + \Psi + \varphi_e(t))}, \tag{5}$$

where $\varphi_e(t)$ is the unknown instantaneous value of the phase error due to phase noise.

Let us consider a signal $x(t)$ similar to $s(t)$ except for one difference; the unknown phase error $\varphi_e(t)$ is replaced by random variable $\Phi(t)$ which represents the uniformly distributed random phases over the time. This means that,

$$x(t) = A_c \mathrm{e}^{j(2\pi f_c t + \Psi + \Phi(t))}. \tag{6}$$

For discrete time $t_n = n\,\Delta t, n = 1,2, \ldots N$, the signal $\xi(t)$ is discretized to get a sequence of N time samples:

$$\xi_n = \xi(t_n) = A_c\, e^{j(2\pi f_c t_n + \Psi)}, \quad n = 1,2, \ldots, N. \tag{7}$$

Initially, a sequence of N uncorrelated uniformly distributed random angles in the closed interval $[-\Phi_{\max}, \Phi_{\max}]$ is generated as follows:

$$\Phi_n = \Phi(t_n) = r_n\, \Phi_{\max}, \tag{8}$$

where r_n is a random number in the range $[-1, 1]$ and $0 < \Phi_{\max} < \pi$.

An expression for the discrete signal x_n can be obtained by adding discrete angle errors Φ_n to the phase of the discrete time samples ξ_n as follows:

$$x_n = x(t_n) = A_c\, e^{j(2\pi f_c t_n + \Psi + \Phi_n)}. \tag{9}$$

Applying the Fast Fourier Transform (FFT) to the discrete sequence x_n, one gets:

$$X_k = X(f_k) = \mathrm{FFT}(x_n), \quad k = 0,1,2, \ldots, K, \tag{10}$$

where $f_k = k\Delta f,\ k = 0,1,2, \ldots, K$, and Δf is the discrete frequency step.

Let's define,

$$\alpha_k = |X_k|, \qquad k = 0,1,2,\dots,K, \tag{11}$$

$$\psi_k = \text{phase}(X_k), \qquad k = 0,1,2,\dots,K. \tag{12}$$

Let us write the discrete form of $L(f)$ as:

$$L(f_k) = L_k, \qquad k = 1,2,\dots,K. \tag{13}$$

To get the desired PSD $L(f)$, the discrete spectrum X_k should be modified by replacing the magnitudes α_k by A_k where,

$$A_0 = A_c, \tag{14-a}$$

$$A_k = \sqrt{P_c\, L_k} = A_c \sqrt{L_k}, \quad k = 1,2,\dots,K. \tag{14-b}$$

Thus, the final form of the carrier $S(f)$ affected by the phase noise signal can be constructed using the magnitudes A_k and the phases ψ_k as follows:

$$S_k = S(f_k) = A_k\, e^{j\psi_k}, \qquad k = 0,1,2,\dots,K. \tag{15}$$

The distribution of the discrete magnitudes of the Fourier transform of a carrier signal affected by the phase noise with the discrete frequencies seems like that shown in Fig. 3. It is worth noting that the spectrum is broadened due to the phase noise and that the carrier power is reduced. It is also important to note that irrespective of the value of $\Phi_{\max}$, the phases ψ_k given by (12) have uniform random distribution in the interval $[-\pi, \pi]$ and the carrier phase is equal to Ψ.

The corresponding time sequence of the carrier signal, can be obtained by applying the Inverse Fast Fourier Transform (IFFT) to the frequency samples, S_k:

$$s_n = s(t_n) = \text{IFFT}(S_k). \tag{16}$$

The discrete-time phase error due to phase noise, φ_{e_n} which is the phase error at each time sample $\varphi_{e_n} = \varphi_e(t_n)$, can be obtained as follows:

$$\varphi_{e_n} = \tan^{-1}\left[\frac{\text{imag}(s_n)}{\text{real}(s_n)}\right] - (2\pi f_c t_n + \Psi). \tag{17}$$

Thus, the discrete time sequences of carrier signal affected by phase noise can be expressed as:

$$s_n = s(t_n) = Ae^{j(2\pi f_c t_n + \Psi + \varphi_{e_n})}. \tag{18}$$

It may be interesting to notice that even though the sequences Φ_n are uncorrelated random samples with time, the samples φ_{e_n} are sequentially correlated. Actually, the correlation effect is attributed to the imposed magnitude distribution, A_k, that replaces the magnitudes α_k corresponding to the uncorrelated sequences.

It may be worth to recall that the number of time/frequency samples for IFFT is restricted by $N = \frac{1}{\Delta f \Delta t}$. The main drawback of this method is that the requirement of 1 Hz resolution of the resulting phase noise model in the frequency domain means the application of IFFT on a huge number of frequency samples. Quantitatively speaking, for $\Delta f = 1$ Hz and assuming the time sampling is to be performed with the Nyquist rate, $\Delta t = 1/2f_c$, one gets:

$$N = 2f_c. \tag{19}$$

It should be noted that (19) gives the minimum value of $\boldsymbol{N}$. Larger values of $\boldsymbol{N}$ result in better accuracy of the obtained model of the phase noise. Nevertheless, this leads to computational complexity which may be unaffordable for high carrier frequency.

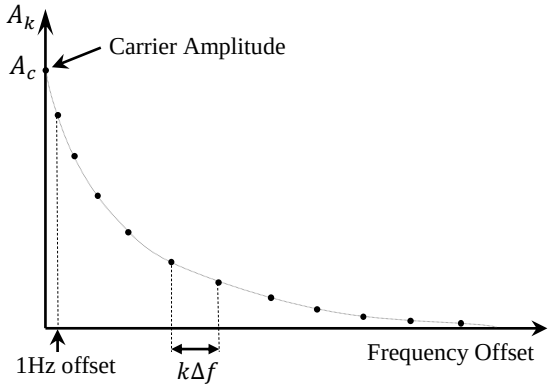

Fig. 3. Magnitudes of the spectrum of the noisy carrier signal, $S(f)$.

B. Modeling phase noise as uncorrelated random phases in the frequency domain

As mentioned above, the method introduced in the previous section leads to high computational complexity for high frequency carrier. In this section, a more computationally efficient method alternative to that described in the last section is introduced. This method starts constructing the phase noise model directly in the frequency domain by generating the phases ψ_k as uniformly distributed random numbers in the range $[-\pi, \pi]$ in one hand, and, in the other hand, using the magnitudes A_k given by (14) to construct the discrete frequency samples S_k as expressed in (15). The phase at the carrier frequency (zero frequency offset) is set equal to phase of the carrier in the absence of phase noise (Ψ).

The discrete frequency domain samples S_k of the carrier signal are constructed using the magnitudes A_k and the random phases ψ_k according to the following expression:

$$S_k = S(f_k) = A_k\, e^{j\psi_k}. \tag{20}$$

At a specific discrete time index, n, the sample s_n can be calculated by applying the Discrete Inverse Fourier Transform (DIFT) as follows:

$$s_n = s(t_n) = \text{DIFT}(S_k). \quad (21)$$

The corresponding phase error φ_{e_n} due to phase noise is calculated using (17). Note that the time step Δt for DIFT calculation is set arbitrarily; it doesn't obey the restriction for the relation between Δf and Δt as in the IFFT. This enables computationally efficient calculation of the phase error samples over a large time span with arbitrary time resolution. Also, this method enables computationally efficient construction of the spectrum of the noisy carrier signal over an arbitrary frequency range centered at the carrier frequency with high frequency resolution (1 Hz).

III. RESULTS AND DISCUSSIONS

Recall that the purpose of constructing a phase noise model is to get complete description of a carrier signal affected by phase noise. In this section, a model is constructed for such a carrier signal given the PSD distribution of the phase noise. Such a model describes the time samples of the carrier as well as the samples of the instantaneous phase errors encountered due to the phase noise. Two oscillators of carrier frequencies 1 MHz and 1 GHz are considered and the corresponding signal models are constructed by following the procedures explained in Sections II.A and II.B, respectively. For each carrier signals, the time samples of the phase error are calculated over a time span of 1 second. For experimental assessment, the frequency-domain method proposed in the present work is applied to obtain the models of the noisy carrier signals output from two commercially available microwave generators. A vector signal analyzer (VSA) is used for measuring the PSD of the encountered phase noise for the two microwave generators. Finally, the performance assessment of M-ary PSK communication systems subjected to phase noise is achieved regarding the BER and SER for $M = 4$ and 8.

A. Modeling phase noise as correlated sequential random phase errors

For carrier signals of relatively low frequency (a few megahertz) affected by phase noise, it is appropriate to apply the method described in Section II.A to construct the phase noise model by correlating random sequence of uncorrelated phases in the time domain. Such uncorrelated random sequence is generated as uniformly distributed random numbers. In the present section, this method is applied to obtain the noise model for a 1 MHz carrier signal affected by phase noise having a predetermined PSD distribution over the frequency.

A.1 Construction of the frequency spectrum magnitudes of the noisy signal

Let the PSD, $L(f)$, for a range of 1 MHz offset from the carrier frequency be that shown in Fig. 4. In the first and second decades: $(1\text{Hz} - 10\text{ Hz})$, $(10\text{ Hz} - 100\text{ Hz})$, the $L(f)$ curve has slopes of -40 and -30 dB/decade, respectively. In the third and fourth decades: $(100\text{ Hz} - 1\text{ kHz})$, $(1\text{ kHz} - 10\text{ kHz})$, it has slope of -20 dB. In the fifth decade: $(10\text{ Hz} - 100\text{ kHz})$, it has slope of -10 dB. For frequencies higher than 100 kHz, the $L(f)$ curve has a zero-slope corresponding to white phase noise level of -130 dBc/Hz. The maximum of the PSD is -10 dBc/Hz at 1 Hz offset from the carrier. If a carrier signal of 1 MHz is affected by phase noise of such a PSD, the corresponding magnitudes of the signal spectrum can be obtained by (14). Figure 5 shows a plot of the resulting signal spectrum magnitudes for a single side span of 100 Hz offset from the carrier frequency.

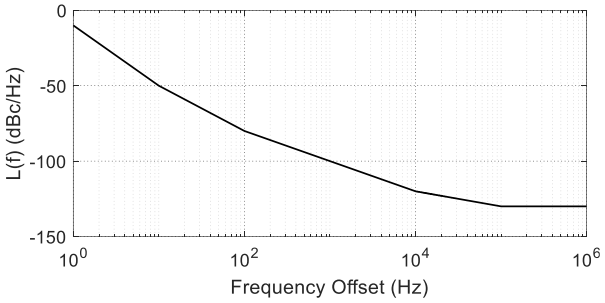

Fig. 4. Power spectral density $L(f)$ of the phase noise.

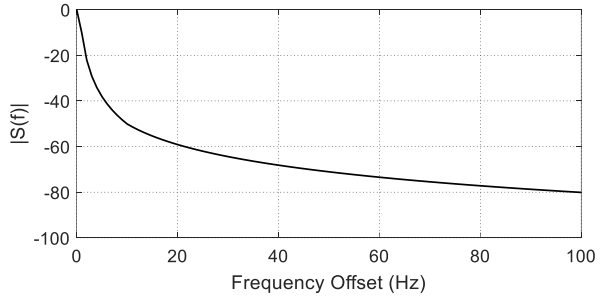

Fig. 5. Amplitude spectrum of the synthesized model, $S(f)$, for a 1 MHz carrier affected by phase noise of the PSD given in Fig. 4.

A.2 Phases of the frequency spectrum of the noisy signal

The time-domain carrier signal is discretized so that each cycle of the sinusoid has 16 time samples. Thus, for one second duration of this signal, the total number of samples is $N = 16\text{M}$ samples with time resolution of $\Delta t = \frac{1}{N}$ (as $\Delta f = 1\text{Hz}$). The uncorrelated uniformly distributed random sequence of phase samples $\Phi(t)$ are generated as described in section II.A according to (8) with $\Phi_{\max} = \frac{\pi}{2}$. The application of the FFT operation on the discrete-time carrier signal x_n given by (9) with the imposed phase samples, Φ_n, results in a spectrum whose magnitudes and phases in the frequency domain are α_k and ψ_k, respectively. The phases, ψ_k, are found to be random numbers which are uniformly distributed in

the range $[-\pi, \pi]$. The plot of such phases with the frequency is presented in Fig. 6 for an offset frequency span of 100 Hz from the carrier frequency.

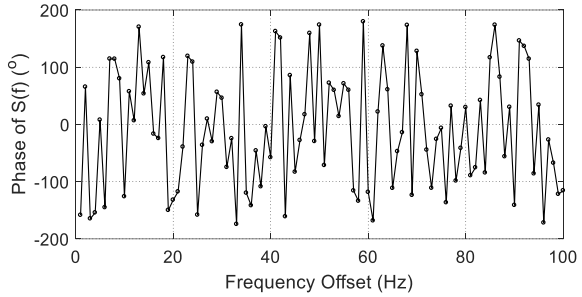

Fig. 6. Distribution of the discrete phases of $S(f)$ with the frequency for a carrier signal affected by phase noise.

A.3 The phase error time samples

It should be mentioned that the phase error is calculated by continuing the steps achieved in Section A.2, according to the procedure explained in Section II.A. The α_k magnitudes are, then, replaced by A_k which are given by (14) to obtain the frequency spectrum, $S_k \equiv S(f_k)$, of the noisy carrier signal as described by (15). The IFFT is, then, applied to the discrete frequency samples, S_k, to get the discrete time samples $s_n \equiv s(t_n)$. The time samples of the instantaneous phase error φ_{e_n} are obtained using (17). The calculated time samples of φ_{e_n} for a time span of one second are plotted against the time and shown in Fig. 7. It is clear that the sequential samples of the phase error are temporally correlated over the one-second span of the time. The swing of the phase error, which is the difference between the maximum and minimum, is about 65°.

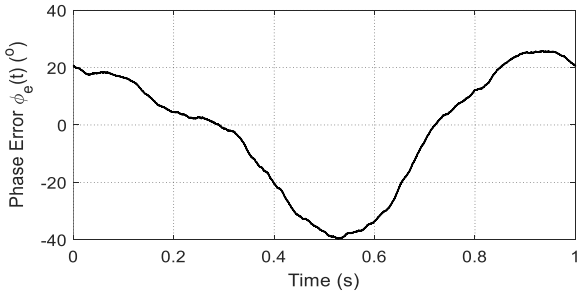

Fig. 7. Time samples of the instantaneous phase error of a carrier signal affected by phase noise of the PSD described by the curve $L(f)$ presented in Fig. 4 with $\Psi = 0°$.

B. Modeling phase noise as uncorrelated random phases in the frequency domain

For carrier signals of relatively high frequency (gigahertz) affected by phase noise, it is appropriate to apply the method described in Section II.B to construct the phase noise model by generating uncorrelated random sequence of phases in the frequency domain. In the present section, this method is applied to obtain the phase noise model for a 1 GHz carrier signal of 0dBm power and 0° phase. This signal is affected by phase noise of the PSD distribution presented in Fig. 4 which is defined over the frequency offset range 1 Hz to 1 MHz with a frequency step $\Delta f = 1$ Hz.

The spectrum of the noisy signal is obtained by calculating the distribution of the magnitudes and phases over the frequency range $(f_c - 1\text{ MHz})$ to $(f_c + 1\text{ MHz})$. The magnitudes are obtained from the PSD distribution, $L(f)$, as given by (14) and by setting $A_{-k} = A_k$ to get symmetrical sidebands. This results in the magnitudes distribution presented in Fig. 8 over the offset frequency range (−4 kHz to 4 kHz) from f_c.

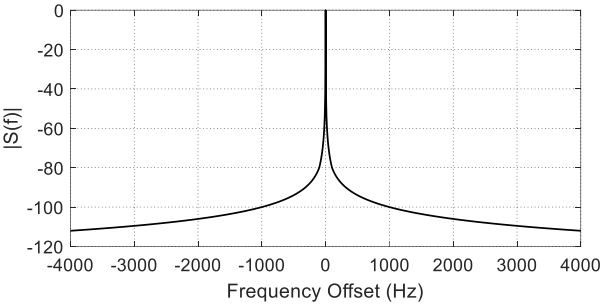

Fig. 8. Magnitudes of the spectrum for a 1 GHz carrier signal affected by phase noise of the PSD distribution presented in Fig. 4.

It should be noticed that to cover the entire frequency band, $(f_c - 1\text{ MHz})$ to $(f_c + 1\text{ MHz})$, a number of 2 mega samples of the frequency samples plus the carrier frequency sample are required. The frequency domain phases, ψ_k, are generated as uniformly distributed random numbers in the interval $[-\pi, \pi]$.

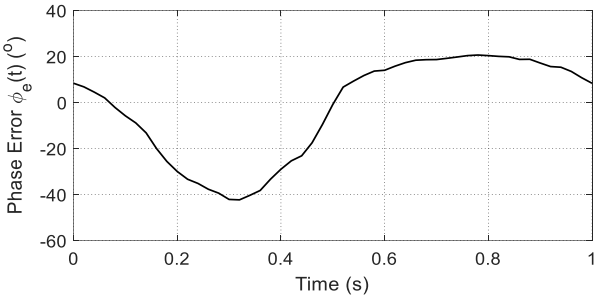

Fig. 9. Calculated instantaneous phase error for a 1 GHz carrier due to phase noise with the PSD shown in Fig. 4.

The phase error at each time sample is calculated as given by (17) with time step $\Delta t = 5$ms and plotted over a time period of one second as shown in Fig. 9. It can be seen in the figure that the mean of the phase error is 0° and the swing is about 65°. The time samples φ_n are

calculated over a time span of one second.

C. Dependence of the time-variance of the phase error on phase noise power

It has been shown, in the previous discussions of the results concerning the time variation of the phase error, that it can be considered as a time-correlated sequence of random angles with zero-mean and a variance that may be dependent on the power of the phase noise. The dependence of the time-variance of the resulting phase error on the power of a phase noise having a spectral density distribution as shown in Fig. 4 and affecting a 1 GHz carrier signal is studied. It may be worth noting that, referring to Fig. 4, the area under the $L(f)$ curve within the operational bandwidth, gives half the ratio of noise power to the carrier power. In Fig. 10 the standard deviation of the phase error and the corresponding span are calculated for different NCR within a 10 MHz bandwidth for a 1 GHz carrier frequency having 0 dBm power. It is clear that as the NCR increases the phase error variance and, consequently, its span increase monotonically.

D. Experimental assessment for phase error variance for commercially available oscillators

Experimental data are usually plotted on log-log scales that make the power laws appear as straight lines where the slopes and, hence, the corresponding types of noise can be easily recognized. In this section, the phase noise associated with some commercially available oscillators are measured and modeled to obtain the time samples of the oscillator output.

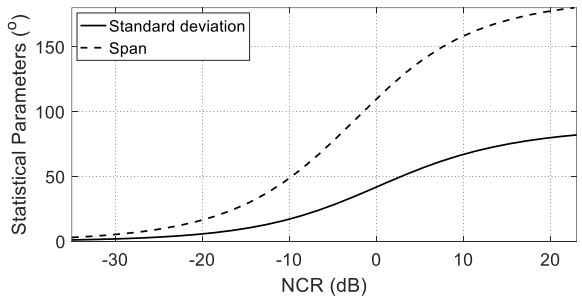

Fig. 10. Span and standard deviation of the phase error for different values of the carrier-to-noise power ratio.

D.1. Modeling the phase noise of the Agilent Vector Signal Generator (VSG) E8267D

The Agilent VSG model E8267D is precise, well-fabricated and commercially available for scientific research purposes. It operates in the frequency band 250 KHz to 44 GHz. The spectrum of the output signal and the phase noise PSD for 1 GHz frequency and 0 dBm power are measured using the Agilent Vector Signal Analyzer (VSA) model N9010A. The experimental setup is shown in Fig. 11 where the E8267D output is connected to N9010A input through a Pasternack coaxial cable PE300-24 (cable length: 60 cm, insertion loss 0.36 dB/m at 1GHz). The phase noise is measured in the offset frequency range 1Hz − 1MHz from the carrier frequency. Front-panel screen shots of the VSG and VSA showing the settings and measurement data are shown in Figs. 12 (a) and 12 (b), respectively. The measured raw data and the averaged curve of the phase noise are plotted as shown in Fig. 13. The spectrum of the output signal is measured using the VSA with resolution bandwidth (RBW) of 1 Hz and video bandwidth (VBW) of 1 KHz over a 100 Hz span. The measured power spectrum is plotted as shown in Fig. 14.

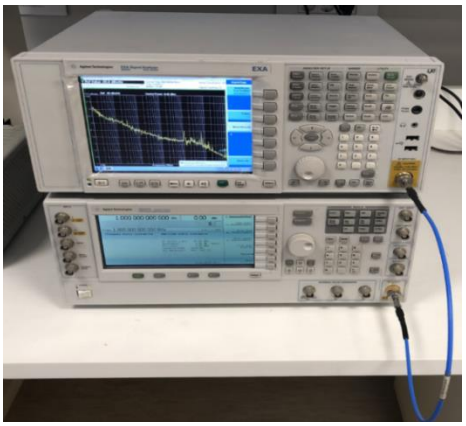

Fig. 11. Experimental setup for measuring the phase noise of the Agilent VSG model E8267D.

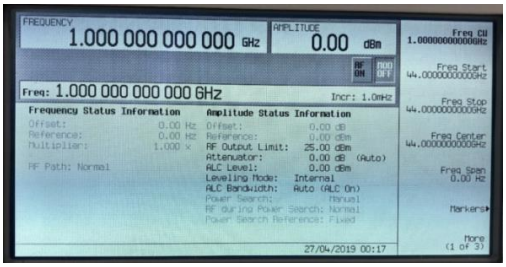

(a)

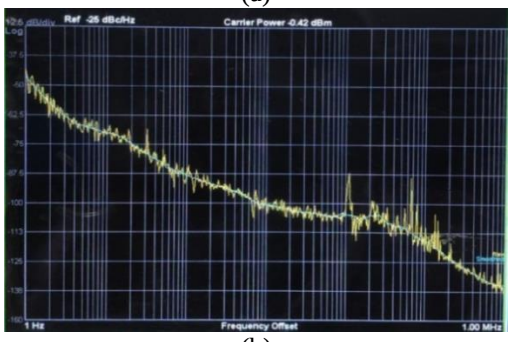

(b)

Fig. 12. Screen shots of (a) VSG E8267D showing the oscillator settings, and (b) VSA N9010A, showing the corresponding phase noise measurements.

The power spectrum of the output signal from such a VSG can be calculated from the PSD of the associated phase noise over a span of 100 Hz using (14) as described in Section II.A. In this way, the measured PSD of phase noise shown in Fig. 13, is used to numerically obtain the power spectrum of the output signal which is plotted and compared with the measured spectrum as shown in Fig. 14. As shown in the figure the calculated power spectrum agrees with the measured one over the entire frequency band, which ensures the accuracy of the developed model.

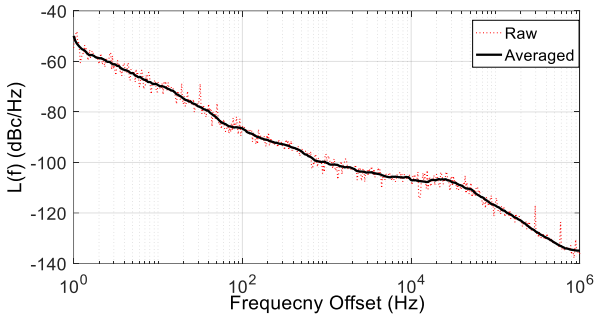

Fig. 13. Measured PSD of the phase noise for Agilent VSG model E8267D for 1 GHz frequency and 0 dBm power.

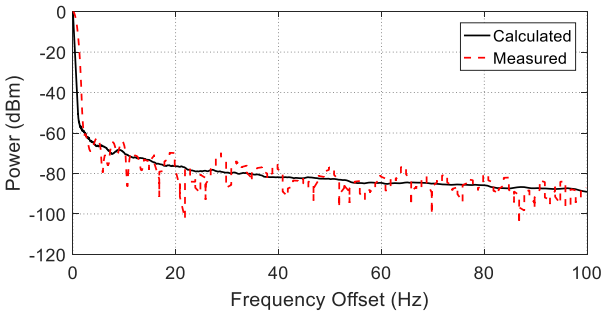

Fig. 14. Power spectrum of the 1 GHz, 0 dBm output signal of the Agilent VSG model E8267D.

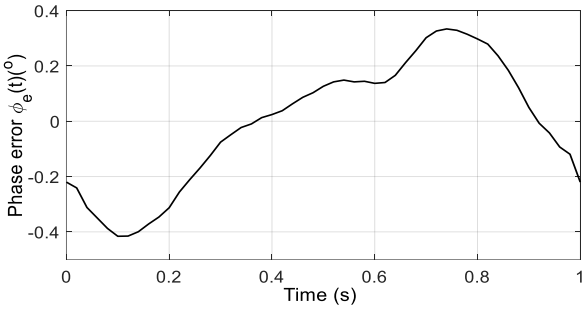

Fig. 15. Instantaneous phase error associating the output signal of the Agilent VSG model E8267D.

Following the procedure explained in Section II.B, the magnitudes A_k of the spectrum is obtained from the measured phase noise PSD shown in Fig. 13. On the other hand, the phases ψ_k are generated as uniformly distributed random numbers in the interval $[-\pi, \pi]$. The DIFT is applied to the constructed signal spectrum to get the time samples of the phase error over a time span of 1 second with resolution $\Delta t = 5$ms. The results are plotted in Fig. 15.

It is clear that the Agilent VSG model E8267D has very low level of phase noise and, consequently, the span of the phase error is about 0.7° and the corresponding variance is 0.02.

D.2 Modeling the phase noise of the Agilent SG N9310A

The Agilent SG model N9310 is commercially available and operates in the frequency band 9 KHz to 3 GHz. The PSD of the phase noise associating an output signal of 1 GHz frequency and 0 dBm power is measured in the offset frequency range $1\text{Hz} - 1\text{MHz}$ using the same experimental setup described in Section III.D.1 and shown in Fig. 16. The measured data of the phase noise and the averaged curve are plotted as shown in Fig. 17. The instantaneous phase error is obtained from the PSD of the phase noise using the procedure explained in Section II.B and is plotted versus time as shown in Fig. 18.

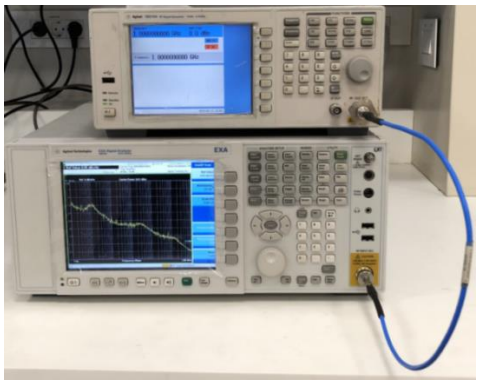

Fig. 16. Experimental setup for measuring the phase noise of the Agilent SG model N9310.

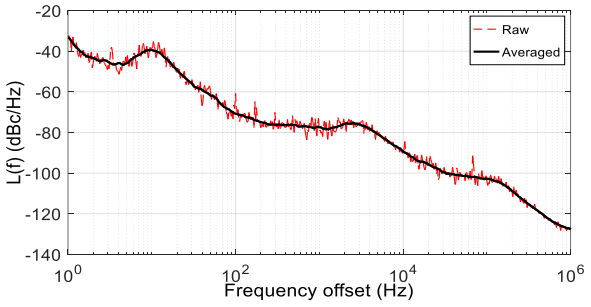

Fig. 17. Measured PSD of the phase noise for Agilent SG model N9310 for an output signal of 1 GHz frequency and 0 dBm power.

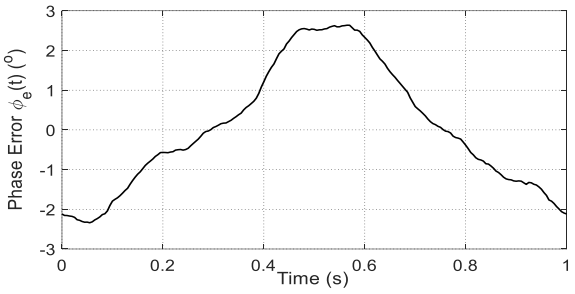

Fig. 18. Instantaneous phase error associating the output signal of the Agilent SG model N9310 for a frequency of 1 GHz and output power of 0 dBm.

E. Performance assessment of M-ary PSK communication systems using the proposed model of the phase noise

In this section, the proposed phase noise model is used to assess the performance of the communication systems employing M-ary PSK modulation techniques in the presence of phase noise. The swing of the instantaneous phase error obtained as described in Section II is used to study the effect of the phase noise on the BER for different levels of the noise power. The procedure is performed with 1 Hz frequency resolution. It should be noted that, in the following presentations and discussions, the phase noise is assumed to have the PSD described in Fig. 4. The BER and SER are calculated for $M = 4$ and 8 at different values of the NCR through numerical simulation of the communication process where 10 M symbols are to be received. The symbol rate is assumed to be 10 Msps. The time samples of the phase error are obtained for each value of the NCR following the procedure explained in Section II.B. At the time of receiving a symbol, the instantaneous value of phase error is added to the phase of this symbol. The calculated BER and SER for $M = 4$ and 8 are plotted versus the NCR as shown in Figs. 19 and 20, respectively. The constellation diagrams are plotted in Figs. 21 and 22 for phase error spans of 20^o ($NCR \approx -28\ dB$) and 30^o ($NCR \approx -22\ dB$), respectively for M-ary PSK systems with $M = 4$ and 8.

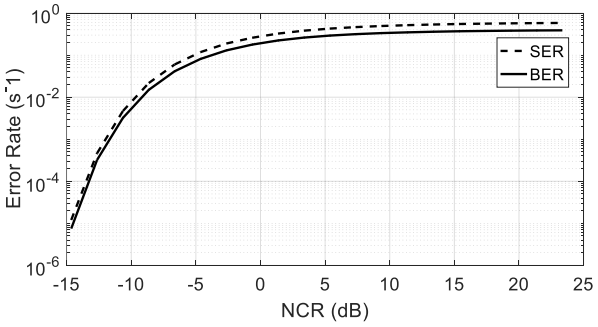

Fig. 19. BER versus NCR for M-ary PSK system with $M = 4$.

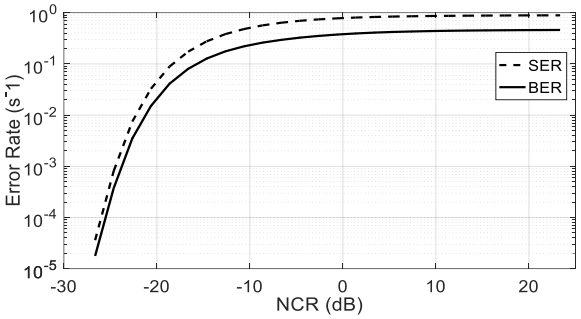

Fig. 20. BER versus NCR for M-ary PSK system with $M = 8$.

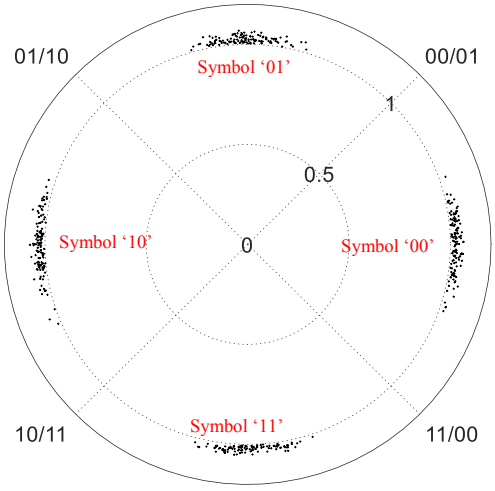

(a)

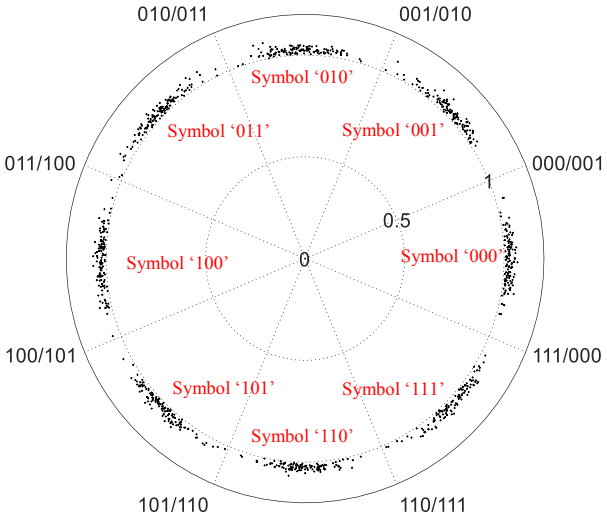

(b)

Fig. 21. Constellation diagram for M-ary PSK system affected by phase noise at phase error swing of 20^o: (a) $M = 4$ and (b) $M = 8$.

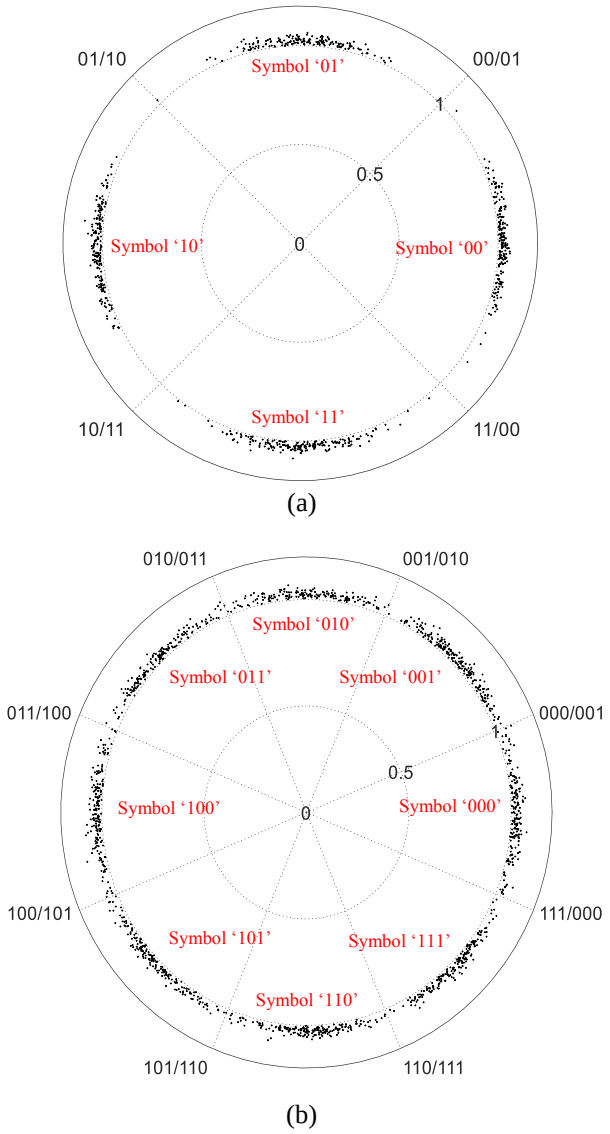

Fig. 22. Constellation diagram for M-ary PSK for phase error range of 30^o: (a) $M = 4$ and (b) $M = 8$.

IV. CONCLUSION

Numerical models of the oscillator phase noise using two mathematical procedures to calculate the resulting instantaneous phase error are introduced. Experimental measurements of the PSD of the phase noise encountered in some commercially available oscillators have been performed and the time samples of the corresponding phase error are calculated. To demonstrate the importance and applicability of the proposed model of the phase noise, the effect of the resulting phase error on some performance measures of the M-ary PSK modulation techniques, such as the SER and BER, is investigated for $M = 4$ and 8.

REFERENCES

[1] M. Reza Khanzadi, "Phase Noise in communication Systems Modeling, Compensation, and Performance Analysis", Thesis for degree of Doctor of Philosophy, *Chalmers University of Technology*, Nov. 2015.

[2] Study Programme 3B/7, "Characterization of frequency and phase noise", *International Radio Consultative Committee*, pp. 142-150, 1986.

[3] J. Rutman, "Characterization of phase and frequency instabilities in precision frequency sources: Fifteen years of progress," *Proceeding of the IEEE*, vol. 66, no. 9, Sep. 1978.

[4] M. Jankovic, "Phase Noise in Microwave Oscillators and Amplifiers," *University of Colorado, Department of Electrical, Computer and Energy Engineering*, 2010.

[5] E. Rubiola, E. Salik, S. Huang, N. Yu, and L. Maleki, "Photonic-delay technique for phase-noise measurement of microwave oscillators," *Journal of the Optical Society of America B*, vol. 22, no. 5, pp. 987-997, 2005.

[6] M. Reza. Khanzadi, "Modeling and Estimation of Phase Noise in Oscillators with Colored Noise Sources," Thesis for degree of Licentiate of Engineering, *Chalmers University of Technology*, August 2013.

[7] F. Brandonisio and M. P. Kennedy, *Noise Shaping all Digital Phase Locked Loops*, ch. 7, Springer 2014.

[8] J. A. Barnes and D. W. Allan, "A statistical model of flicker noise," *Proceedings of the IEEE*, vol. 54, no. 2, Feb. 1966.

[9] J. J. Podesta, "Phase noise cancellation in a mixer ciruit: Analysis using a random phase function," *Technical Report ARFSD-TR-95016*, Jan. 1996.

[10] A. Demir, A. Mehrotra, and J. Roychowdhury, "Phase noise in oscillators: A unifying theory and numerical methods for characterization," *IEEE Transactions on Circuits and Systems-I: Fundamental Theory and Applications*, vol. 47, no. 5, May 2000.

[11] P. Vu, A. M. Haimovich, and B. Himed, "Effect of phase noise on spatial processing by sensors with independent oscillators," *IEEE Radar Conference*, 2018.

[12] C. Mathai, S. A. Bhave, and S. Tallur, "Modeling the colors of phase noise in optomechanical oscillators," *OSA Continuum*, vol. 2, no. 7, July 2019.

[13] D. A. Howe, "Frequency domain stability measurements: A tutorial introduction," *National Bureau of Standards (NBS)*, Technical Note 679, Mar. 1976.

[14] R. F. Lacey, A. L. Helgesson, and J. H. Holloway, "Short-Term stability of passive atomic frequency standards," *Proceedings of the IEEE*, vol. 54, no. 2, Feb. 1966.

[15] D. Halford, A. E. Wainwright, and I. A. Barnes, "Flicker noise of phase in RF amplifiers and frequency multipliers: Characterization, cause and cure," (summary), in *Proc. 22nd Annu. Frequency Control Symp*., Atlantic-City, NJ, pp. 340-341, Apr. 1968.

[16] L. Dickstein "Introduction to phase noise in signal generators," white paper, *Giga-Tronics*, 2012.

[17] A. Hajimiri and T. H. Lee, "A general theory of phase noise in electrical oscillators," IEEE Journal of Solid-State Circuits, vol. 33, no. 2, Feb. 1998.